minerals MDPI

Article

Revealing the Softening-Melting Behaviors and Slag Characteristics of Vanadium-Titanium Magnetite Burden with Various MgO Addition

Bin Wang [1,2], Wei Zhao [1,*], Xinghua Zhang [3], Shaoyan Hu [1,*], Hongwei Guo [1] and Mansheng Chu [3]

1 School of Iron and Steel, Soochow University, Suzhou 215137, China; wang_bin919@126.com (B.W.); guohongwei@suda.edu.cn (H.G.)
2 Central Iron and Steel Research Institute, Beijing 100081, China
3 School of Metallurgy, Northeastern University, Shenyang 110819, China; lionzxh@163.com (X.Z.); chums@smm.neu.edu.cn (M.C.)
* Correspondence: zhaowei0312@suda.edu.cn (W.Z.); syhu616@suda.edu.cn (S.H.)

Abstract: MgO addition plays an essential role in the blast furnace smelting process, including softening-melting characteristics and metallurgical properties of slag. In the present study, the effect of MgO distribution on the softening-melting characteristics and slag system of vanadium-titanium magnetite burden were explored by simulating BF conditions. The results show that the MgO flux addition significantly affects the crystallization temperature of slag-phase, the precipitated phase components, and slag viscosity. This indicates that appropriate MgO addition can improve the metallurgical properties of blast furnace slag effectively, thereby improving the softening-melting-dripping performance of the mixed burden. The V-Ti pellets with a MgO content higher than 2.40 wt% exhibit optimum metallurgical properties. With a constant MgO content in mixed burden, the softening-melting properties of composite burden could be improved effectively as the MgO partitioning scheme includes 1.90 wt% MgO in sinter and 3.02 wt% MgO in pellet.

Keywords: MgO; V-Ti composite burden; softening-melting characteristics; slag-phase; blast furnace

check for updates

Citation: Wang, B.; Zhao, W.; Zhang, X.; Hu, S.; Guo, H.; Chu, M. Revealing the Softening-Melting Behaviors and Slag Characteristics of Vanadium-Titanium Magnetite Burden with Various MgO Addition. *Minerals* **2022**, *12*, 842. https://doi.org/10.3390/min12070842

Academic Editor: Mark I. Pownceby

Received: 30 May 2022
Accepted: 28 June 2022
Published: 30 June 2022

1. Introduction

Vanadium-titanium magnetite (VTM) is a vital metallurgical raw material [1,2]. There is approximately more than 18 billion tons of VTM deposit in Panxi district and Chengde district of China. The main utilization method of VTM in China is still the blast furnace ironmaking process, in which sinter is the dominant iron-bearing raw material [3–6]. However, in the process of smelting vanadium-titanium composite burden in the blast furnace, there are still some urgent problems, such as softening-melting characteristics, low permeability index, poor slag flow performance, low V yield, and so on [7–9].

MgO content has a significant impact on the quality of sinter and pellet [10–12]. Appropriate MgO content can enhance the stability, fluidity and metallurgical properties of slag and improve the desulfurization capacity of slag [13,14]. Charging the iron-bearing raw materials with various MgO addition is a direct and effective measure to adjust the content of MgO in final slag and improve the smelting conditions of the cohesive zone in the blast furnace [15,16].

The influence of MgO on sinter and pellet has been studied for many years [17–21]. Large amounts preceding works demonstrated that adding MgO in pellet or sinter could enhance its high temperature properties. Zhao [22] observed that the softening-melting behavior and permeability of V-Ti pellets packed bed were improved with increasing MgO content. Umadevi T [23] studied the effect of MgO on reducibility and softening-melting behaviors of sinters. It was found that the addition of dolomite, which contains a lot of MgO, will optimize the reducibility and softening-melting behavior of sinters. Higuchi et al. [24]

highlighted that when the sinter had low Al_2O_3, high MgO, and 1.0–1.5 basicity, the T_S and T_D is the best. Guo et al. [25] considered that the reduction behavior was inhibited by the increase in MgO content through the study on the high-temperature reduction and melting mechanism of sinters with various MgO content.

At present, the research on the influence of MgO on the smelting process mostly focuses on sinter or pellet. In the present study, the impact of MgO apposition on the softening-melting performance and properties of blast furnace slag were investigated systematically with simulating blast furnace conditions. Firstly, the softening-melting behaviors of V-Ti composite burden with various MgO partitioning schemes were explored systematically by conducting softening-melting-dripping tests. Simultaneously, the impact of MgO on the softening-melting behavior of V-Ti pellet was studied to compare with that of mixed burden. Finally, the impact of varying MgO content on the metallurgical performance of blast furnace slag was studied to illuminate the softening-melting characteristics of composite burden. Finally, the optimal production parameters were determined by coupling the softening-melting behavior and metallurgical performance of slag.

2. Experimental

2.1. Raw Materials

To explore the impact of MgO distribution on the softening-melting behavior of mixed burden, the proportions of sinters, pellets, and lump ore were 70:22:8, which simulated the on-site production conditions. The chemical compositions of the V-Ti sinter and pellet with various MgO addition are listed in Table 1. Furthermore, the impact of MgO on the softening-melting behaviors of single V-Ti pellets were explored. In this part, the V-Ti pellet samples were prepared in laboratory, and its chemical compositions are listed in Table 2. All reagents used to synthesis slag were pure chemical reagents, and the diameter of all reagents are below 200 mesh.

Table 1. The chemical compositions of V-Ti sinter and pellet.

Raw Materials	Items	TFe	CaO	SiO_2	MgO	Al_2O_3	TiO_2
Sinter	1#	54.65	10.55	4.91	1.70	1.92	1.88
	2#	54.55	10.57	4.92	1.80	1.93	1.88
	3#	54.46	10.59	4.93	1.90	1.94	1.88
	4#	54.37	10.60	4.93	2.00	1.94	1.87
Pellet	1#	59.08	0.81	5.80	3.63	1.37	1.34
	2#	59.27	0.81	5.82	3.32	1.37	1.35
	3#	59.46	0.81	5.84	3.02	1.38	1.35
	4#	59.66	0.82	5.86	2.71	1.38	1.36

Table 2. Chemical compositions of V-Ti pellet.

Items	TFe	CaO	SiO_2	MgO	Al_2O_3	TiO_2
5#	61.78	0.89	6.54	1.18	1.30	1.45
6#	61.40	0.85	6.25	2.38	1.32	1.48
7#	60.71	0.85	6.18	3.55	1.36	1.49

The chemical composition of the slag, derived from the actual vanadium titanomagnetite blast furnace slag, is listed in Table 3. In this study, the content of MgO is adjusted from 6% to 14% to illuminate the effect of MgO addition on the titanium-bearing slag behaviors. Five analytical pure chemical reagents such as CaO, SiO_2, MgO, Al_2O_3, and TiO_2 are used to synthesize the different slag samples as listed in Table 4. The metallurgical properties of each slag system are measured by an RTW-10 melt physical properties comprehensive tester under a neutral Ar atmosphere. The influence of various components on metallurgical properties of slag was analyzed. In a viscosity furnace, argon was used as the protective atmosphere, and the flow rate was 1.5 L/min. When the slag temperature reached 1500 °C, the constant temperature was kept for 30 min, and then the temperature was reduced to measure the viscosity. The cooling rate was −3 °C/min to obtain the viscosity-temperature (η-t) curves of the slag system.

Table 3. Chemical composition of blast furnace slag on site.

Components	CaO	SiO_2	MgO	Al_2O_3	TiO_2
Content/%	36.02	28.51	9.09	13.16	8.22

Table 4. Chemical composition of blast furnace slag used in the experiment.

Item	CaO/%	SiO_2/%	MgO/%	Al_2O_3/%	TiO_2/%	R_2/-
1	38.89	30.87	6.00	13.16	8.22	1.26
2	37.78	29.98	8.00	13.16	8.22	1.26
3	36.66	29.10	10.00	13.16	8.22	1.26
4	35.55	28,21	12.00	13.16	8.22	1.26
5	34.43	27.33	14.00	13.16	8.22	1.26

2.2. Experimental Methods

The softening-melting furnace was used to investigate the impact of MgO on the softening-melting performance of V-Ti composite burden, as shown in Figure 1a. The dried coke, with a diameter of 10–12.5 mm and a layer thickness of 17 mm and 30 mm was placed over and below the V-Ti composite burden to guarantee the slag and molten iron dropped through and reduction gas passing through. The V-Ti composite burden of approximately 500 g was charged into a graphite crucible with a diameter of 75mm. The composite burden packed bed with various distribution methods of MgO were prepared to be 55 mm. The pressure drop, temperature, and contraction of packed bed during the softening-melting experiment were recorded automatically. Each group of the experimental results of the packed bed were the average of the three experiments. There are 7 groups in total, of which 1#–4# are composite burden and 5#–7# are single pellets.

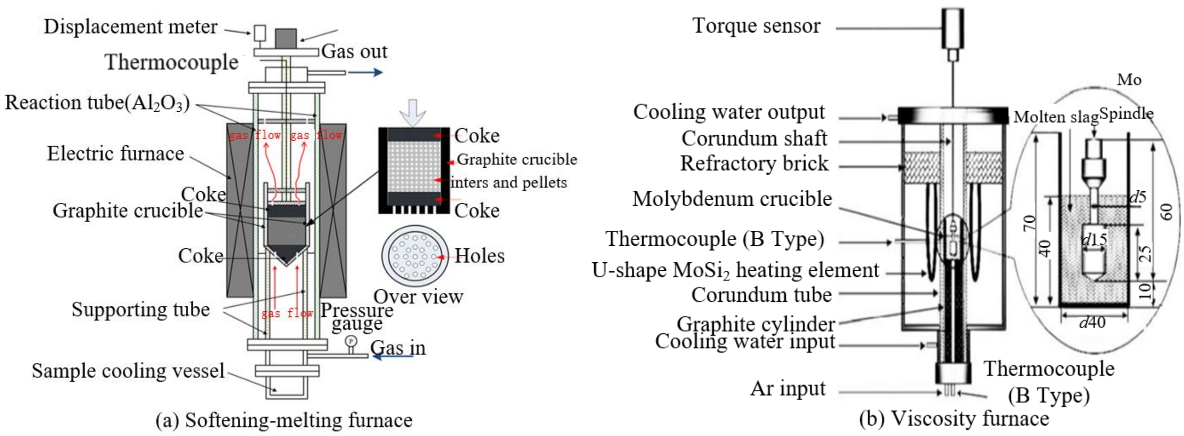

Figure 1. Experimental devices: (**a**) softening-melting furnace; (**b**) viscosity furnace.

The effect of MgO content on the viscosity of the blast furnace slag was tested using a viscosity furnace, as shown in Figure 1b. In order to eliminate the influence of moisture on the quality weighing of vanadium-titanomagnetite blast furnace slag and analysis of pure chemical reagent and reduce the experimental error, the raw materials used in the experiment were roasted and dried. Simultaneously, in order to further simulate the blast furnace production and improve the accuracy of the experimental study, the pre-melting slag of the modulated slag sample was treated to form homogeneous slag. A certain amount of dried CaO, SiO_2, MgO, Al_2O_3, and TiO_2 chemical reagents were mixed with on-site vanadium-titanium blast furnace slag in a certain proportion, and then put into a graphite crucible lined with molybdenum flakes. After that, the graphite crucible was placed in an intermediate frequency induction furnace, and the slag was pre-melted at 1500°C under the condition of Ar gas. After the slag sample was melted for 20 min, the graphite crucible was taken out and the slag sample was cooled. The slag was ground and used for subsequent experiments.

3. Results and Discussion

3.1. Softening-Melting Behavior

The typical results, including the softening start temperature T_4, softening temperature T_{40}, and softening temperature interval (T_{40}-T_4), are shown in Figure 2a. Of particular note is that T_4 and T_{40} were the temperature at which the contraction of packed bed reached 4% and 40%, respectively. Figure 2b shows the melting start temperature Ts, that is, the temperature with a significant increase in pressure drop; the drop temperature T_D, that is, the temperature at which pig iron and slag drop from the graphite crucible; and the melting temperature interval (T_D-T_S).

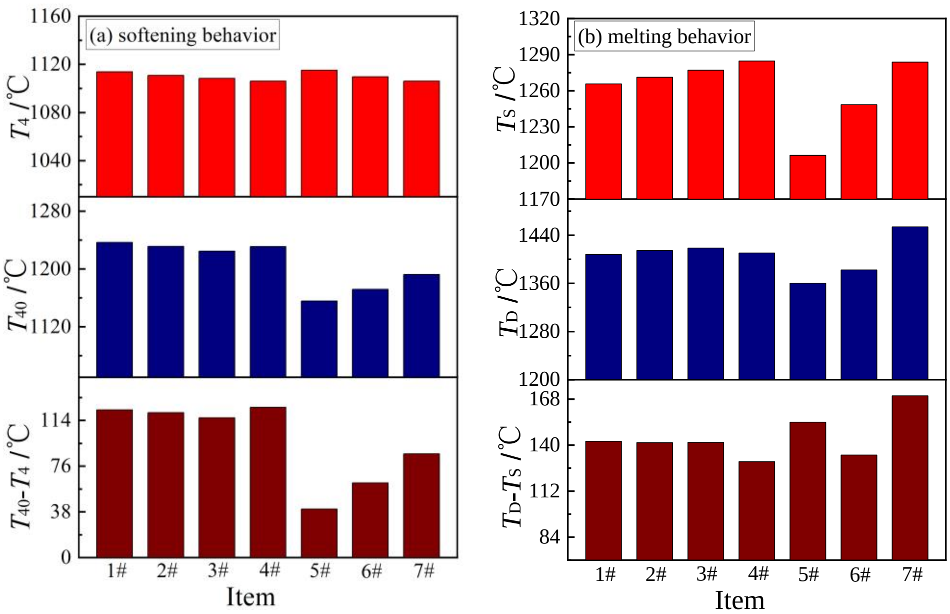

Figure 2. Effect of MgO on softening-melting behavior of V-Ti composite burden and pellets: (**a**) softening behavior, (**b**) melting behavior.

From the test results of 1#–4# groups, with increasing MgO content of V-Ti sinter from 1.7% to 2.0%, T_4 gradually decreased from 1114°C to 1106 °C. T_{40} increased first and then decreased. At the same time, the softening temperature interval (T_{40}-T_4) also increased first and then decreased. From the test results of 5#–7# groups, with decreasing MgO content of V-Ti pellet, T_4 increased gradually, but T_{40} and T_4-T_{40} increased first and then decreased. It should be highlighted that the widening of softening temperature interval could benefit the gas-solid reaction conditions, thereby promoting the reduction of iron-bearing burden.

The typical results of the cohesive zone position and its thickness are shown in Figure 3. From the test results of 1#–4# groups, the position of the cohesive zone shifts down gradually with the increasing content of MgO in sinter when the total content of MgO in the composite burden is constant. In 5#–7# groups of experiments, with the increasing content of MgO in pellet, the same experimental results will appear. It is well known that the shifting down of the cohesive zone position benefits the gas permeability of the blast furnace [7]. Therefore, the increasing MgO content in sinter or pellet is favorable for the gas permeability of V-Ti composite burden.

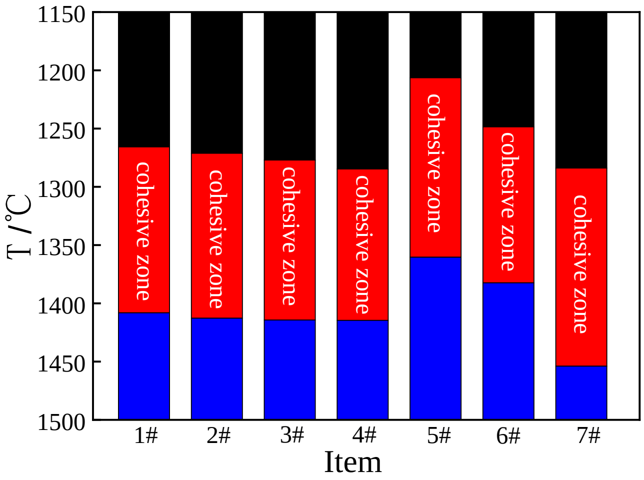

Figure 3. Effect of MgO content on cohesive zone.

The effect of MgO content on the cohesive zone can be explained by the CaO-SiO_2-MgO-Al_2O_3-TiO_2 phase diagram. Figure 4 shows the phase diagram of the primary crystalline region of CaO-SiO_2-MgO-Al_2O_3-TiO_2 isotherm with oxygen partial pressure of 1.0×10^{-5}, in which the contents of Al_2O_3 and TiO_2 are 10.0% and 11.1%, respectively. As it shows that in item 1#–4#, the change of MgO content does not affect the primary crystal field of sinter and pellet, while the primary crystallization temperature of pellet will decrease with the decrease in MgO content. According to the density of isotherm lines, the impact of MgO content in pellet on the primary crystallization temperature of the slag-phase is more obvious than that in sinter when the total MgO content in composite burden is constant. Simultaneously, the enhancement of MgO content could increase the high melting point substances in sinter. Therefore, in group 1#–4#, with the MgO content in sinter increasing and the content of MgO in pellet decreasing gradually, the position of the cohesive zone shifts down, which can be attributed to the sinter and pellet ratio. In group 5#–7#, the primary crystal field and primary crystallization temperature are both changed by MgO content. The primary crystal field of slag moves from the pyroxene region with a low melting point to the olivine region with a high melting point. Hence, with the increase in the MgO content, the T_{40}, $T_{D,}$ and T_S increased.

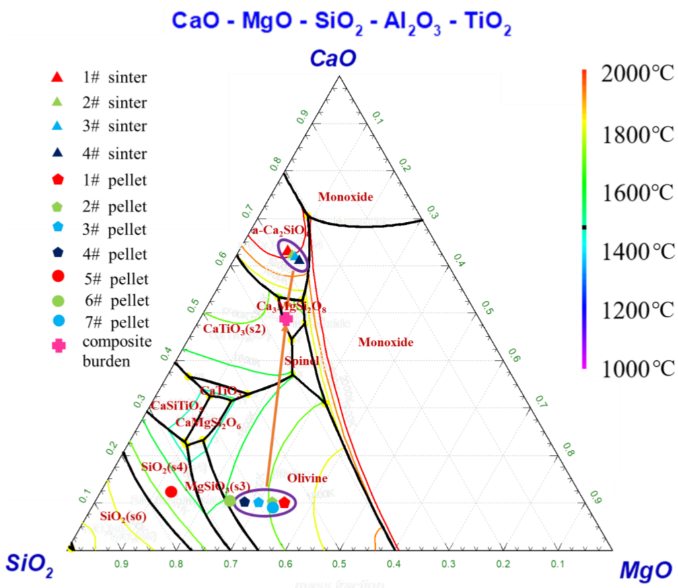

Figure 4. Phase diagram of CaO-SiO_2-MgO (-Al_2O_3-TiO_2) (P = 1atm, $P_{O2} = 1.0 \times 10^{-5}$).

Figure 5 shows the impact of MgO content on the pressure drop of vanadium-titanium magnetite burden packed bed during softening-melting experiments. The sticking and collapse of the packed bed can be restrained by the increase in the high melting point slag, which is conducive to improving the gas permeability. Consequently, with the increase in the MgO content in pellet, the maximum pressure drop is decreased obviously, as shown in Figure 5. In particular, the maximum pressure drop and *S*-value in group 3# and group 4# are basically the same. With the increasing MgO content, the formation amount of slag-phase in sinter and pellet decreases gradually at the same temperature. Generally, the widening of the cohesive zone and the downward movement of the cohesive zone can effectively improve the air permeability of the burden column, thereby reducing the differential pressure of the burden column. Hence, the maximum pressure drop and *S*-value of packed bed are decreasing in group 5#–7#. In group 1#–4#, the liquidus temperature of pellet is decreasing and the liquidus temperature of sinter is increasing. In the composite burden, the content of sinter is much higher than that of pellet. Consequently, the maximum pressure drop and *S*-value of packed bed is decreasing in group 1#–3#. As mentioned above, the effect of MgO content in pellet on the melting point of slag-phase is more obvious than that in sinter. Therefore, the maximum pressure drop and *S*-value of packed bed is basically the same in group 3# and group 4#. In particular, as the sinter proportion in composite burden is much higher than that of pellet in group 4#, the lower melting point of sinter could produce more liquid phase in the composite burden, thereby offsetting the effect of MgO on pellet.

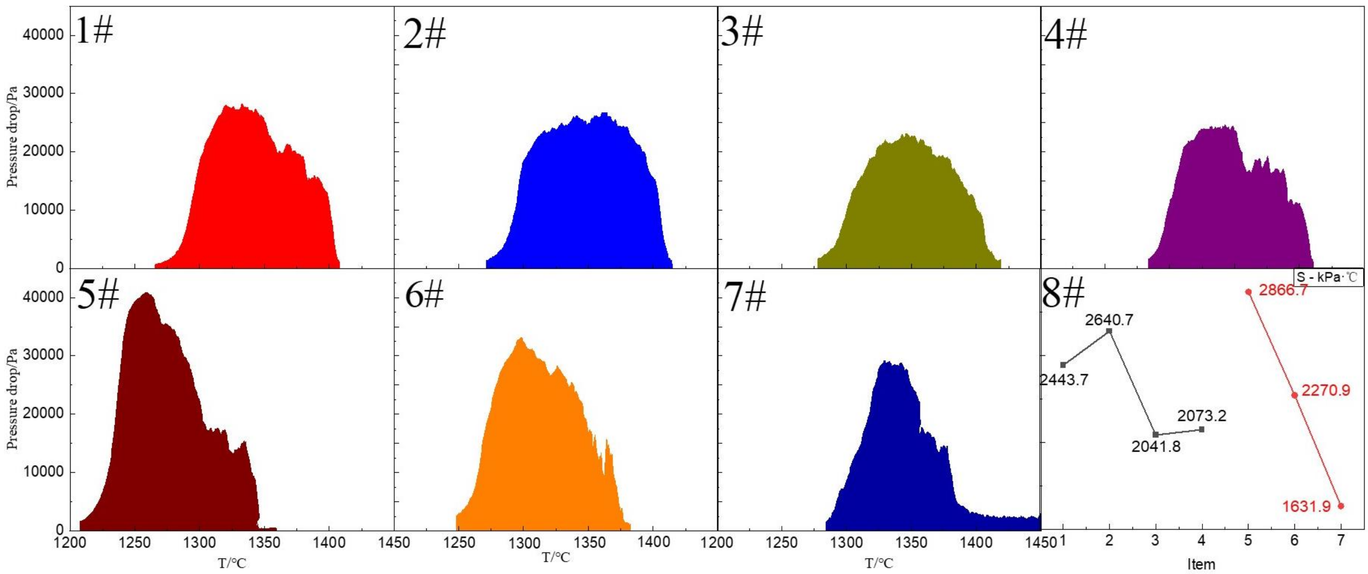

Figure 5. Pressure drop and *S*-value of V-Ti magnetite burden packed bed: (1#–7#) the pressure drop of group 1#–7#, (8#) the *S*-value of group 1#–7#.

The difference in the gas permeability of burden in the blast furnace with different MgO content correlates to the liquid phase formation rate. Figure 6 shows the variation of liquid phase formation rates for various MgO content of V-Ti sinters and pellets. The molten slag generation ratios were calculated by the equilibrium module in FactSage 8.2. It can be seen that the influence of MgO content on the amount of liquid phase in sinter is not obvious at a temperature below 1375 °C, and the MgO content has no obvious effect on the amount of liquid phase at a temperature below 1175 °C. When the temperature is higher than 1400 °C and 1200 °C, the influence of MgO content on the liquid phase formation in sinter and pellet is gradually amplified. What both sinter and pellet have in common is that with the increase in MgO content, the temperature required to produce the same amount of liquid phase increases. It is well known that the premature formation of the liquid phase in the cohesive zone will result in a decrease in the permeability of the burden column and an increase in the differential pressure [22]. Therefore, the improving tendency of the gas permeability of V-Ti burden and pellet could be ascribed to the formation of material with a high melting point.

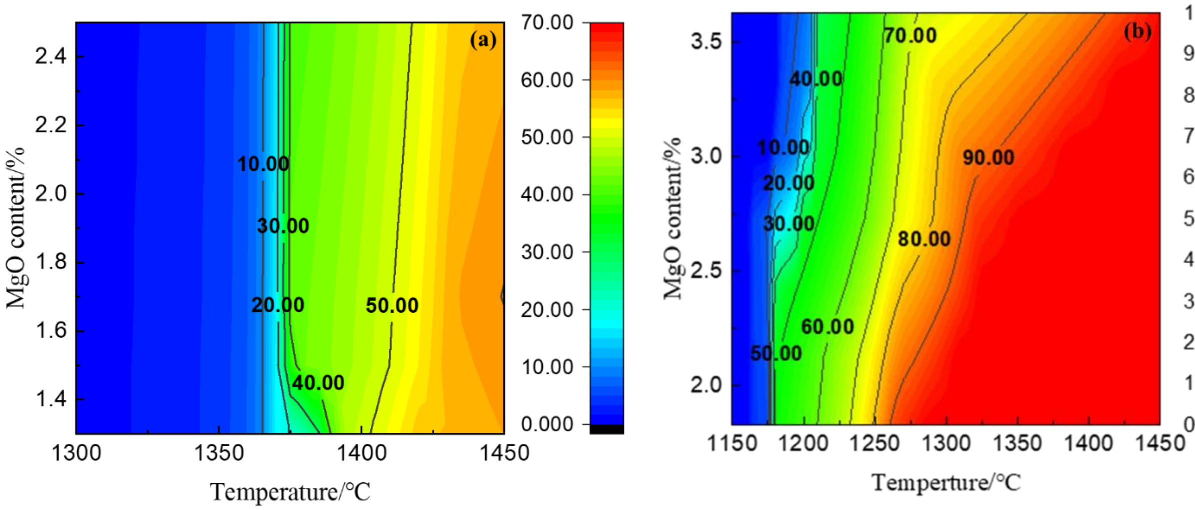

Figure 6. Variation of generation ratio of slag with different MgO content and roasting temperature: (**a**) sinter, (**b**) pellet.

3.2. Effect of MgO on Slag-Phase

The effect of MgO content on viscosity of slag-phase is shown in Figure 7. The MgO slag systems exhibit the characteristics of short slag. With the increase in MgO content, the melting temperature (t_m) and high temperature viscosity (η_h) of the slag system decrease first and then increase, while the initial viscosity (η_0) increases continuously. When the MgO content of slag system is 12.00% and 6.00%, the t_m reaches minimum value of 1333 °C and maximum value of 1348 °C, respectively. When the MgO content is 6.00% and 14.00%, the η_0 reaches the maximum value of 0.845 Pa·s and the minimum value of 0.621 Pa·s, respectively, and the η_h reaches the maximum value of 0.248 Pa·s and the minimum value of 0.172 Pa·s, respectively.

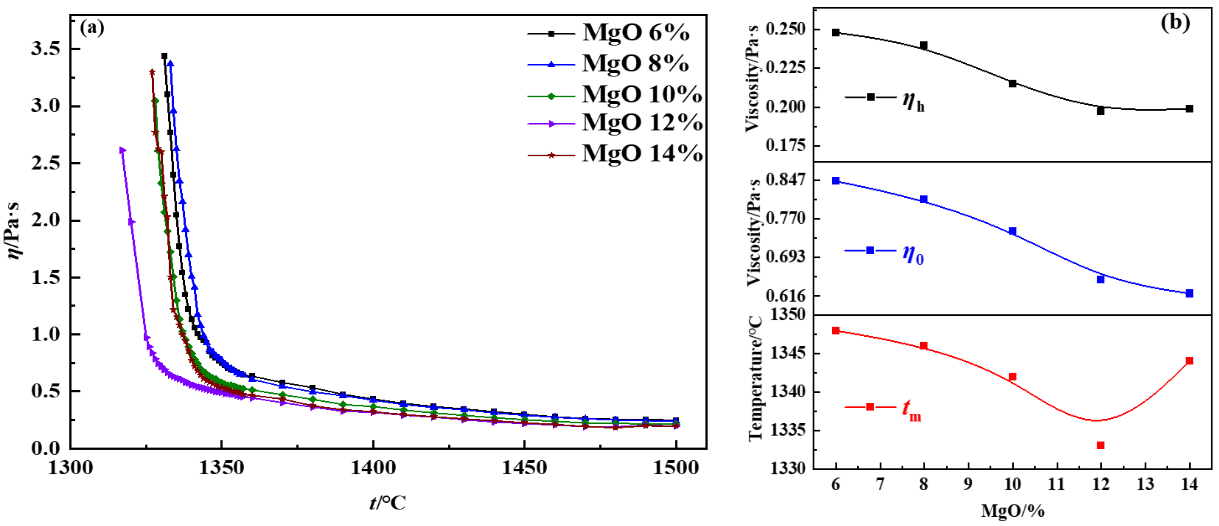

Figure 7. The effect of MgO content on viscosity of slag-phase: (**a**) η-t curves of slag-phase, (**b**) t_m, η_0, η_h of slag-phase.

The viscosity of high temperature slag is mainly determined by its chemical composition, structure, and temperature. In the high temperature slag, the metal cation radius is relatively small, and it has little effect on the fluidity of the high temperature slag, while the silicon–oxygen complex anion $Si_xO_y{}^{z-}$ plays a direct role. $Si_xO_y{}^{z-}$ is the main viscous flow unit in the slag, and the change of the composition of the high temperature slag will cause the disintegration or polymerization of $Si_xO_y{}^{z-}$, resulting in the viscosity decreasing or increasing accordingly. MgO, providing free O^{2-} to high temperature slag, could disintegrate the slag silica–oxygen complex anion $Si_xO_y{}^{z-}$, reduce the viscosity of the slag system to a certain extent, and improve the fluidity of the slag system. Therefore, as the MgO content ranges from 6.00% to 12.00%, with the increase in MgO content in vanadium titanomagnetite high temperature slag, the silicon–oxygen composite anion $Si_xO_y{}^{z-}$ in the slag continues to disintegrate, and t_m, η_0, and η_h show a downward trend. Simultaneously, with the continuous increase in MgO content, the generation of high melting point substances, such as magnesium aluminum spinel ($MgO{\cdot}Al_2O_3$, melting point 2135 °C), would be promoted in the slag. The crystallization ability of the slag system becomes stronger at high temperature, and it is easy to produce the heterogeneous phase in the slag. When the MgO content continues to increase, t_m and η_h show an upward trend.

The viscous flow activation energy can reflect the sensitivity of slag viscosity to temperature. Viscous flow activation energy can be calculated according to the Weymann–Frenkel Equation (1).

$$H = AT\exp(E\eta/RT) \tag{1}$$

η—viscosity, Pa·s;
T—thermodynamic temperature, K;
A—preexponential factor;
$E\eta$—viscous flow activation energy, kJ/mol;
R—gas constant, 8.314 J/(mol·K)
Take logarithms on both sides of the previous equation:

$$\ln(\eta/T) = \ln A + E\eta/RT \tag{2}$$

Substitute the experimental data according to $\ln(\eta/T) - 1/T$ plot and carry out regression treatment, as shown in Figure 8a. The product of slope and R is the viscous flow activation energy of the slag system, as shown in Figure 8b.

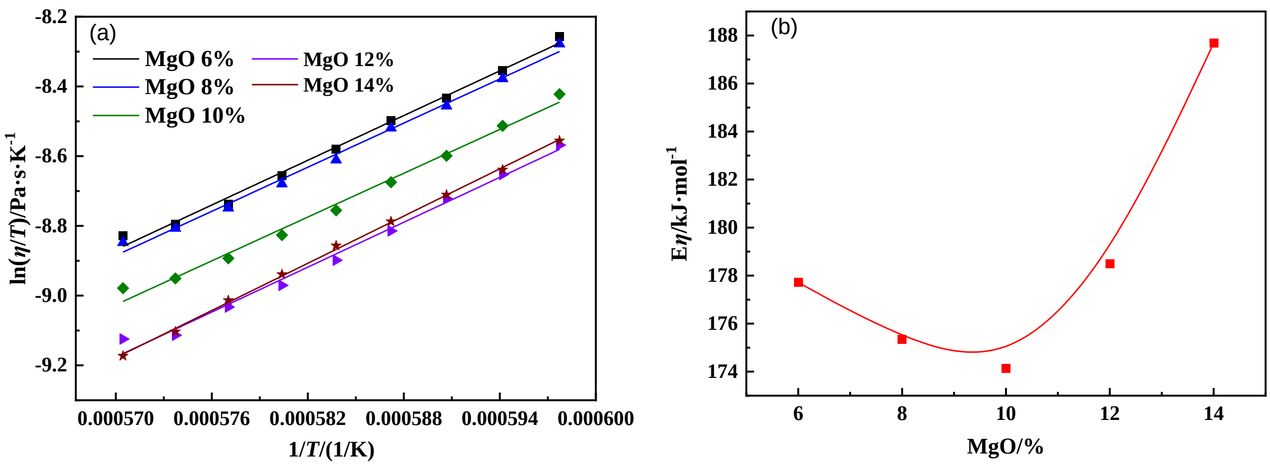

Figure 8. Effect of MgO content on activation energy of viscous flow: (**a**) $\ln(\eta/T) - 1/T$ diagram, (**b**) viscous flow activation energy of various MgO content.

With the increase in MgO content, the viscous flow activation energy of vanadium titanomagnetite high-temperature slag system first decreases and then increases, ranging from 174.13 kJ·mol^{-1} to 187.68 kJ·mol^{-1}. The sensitivity of viscosity to temperature fluctuation first weakens and then enhances, and the thermal stability of the slag system first improves and then deteriorates. With the increase in MgO content, the main viscous flow unit $Si_xO_y^{z-}$ of molten slag disintegrates, and the thermal stability of the slag system becomes better. However, with the further increase in MgO content, the high melting point substances such as magnesia-alumina spinel in the slag increase, which would worsen the thermal stability of the slag system.

To investigate the impact of MgO on the phase change of slag during cooling, a thermodynamics calculation was conducted using Factsage 8.2, as shown in Figure 9. It can be seen that the final amount of melilite increased first and then decreased. The initial formation temperature of melilite increases first and then decreases, and the formation rate becomes faster. The formation amount of spinel increases, and the formation rate becomes faster when the MgO content is increasing. This can be explained by the increase in MgO activity in slag when the MgO content increases, which is conducive to the formation of spinel. The initial formation temperature of perovskite decreases with the increase in MgO content, which results in the formation rate becoming faster and the formation amount gradually increasing at the initial stage of the slag crystallization process. The perovskite formation promotion is due to the fact that the free O^{2-} is conducive to the formation of the perovskite phase, and its amount in slag increases with the increase in MgO content. However, due to the limitation of the TiO_2 content in slag, the final amount of perovskite phase in slag remains unchanged. The formation of pyroxene only occurred when the MgO content is 10.00%.

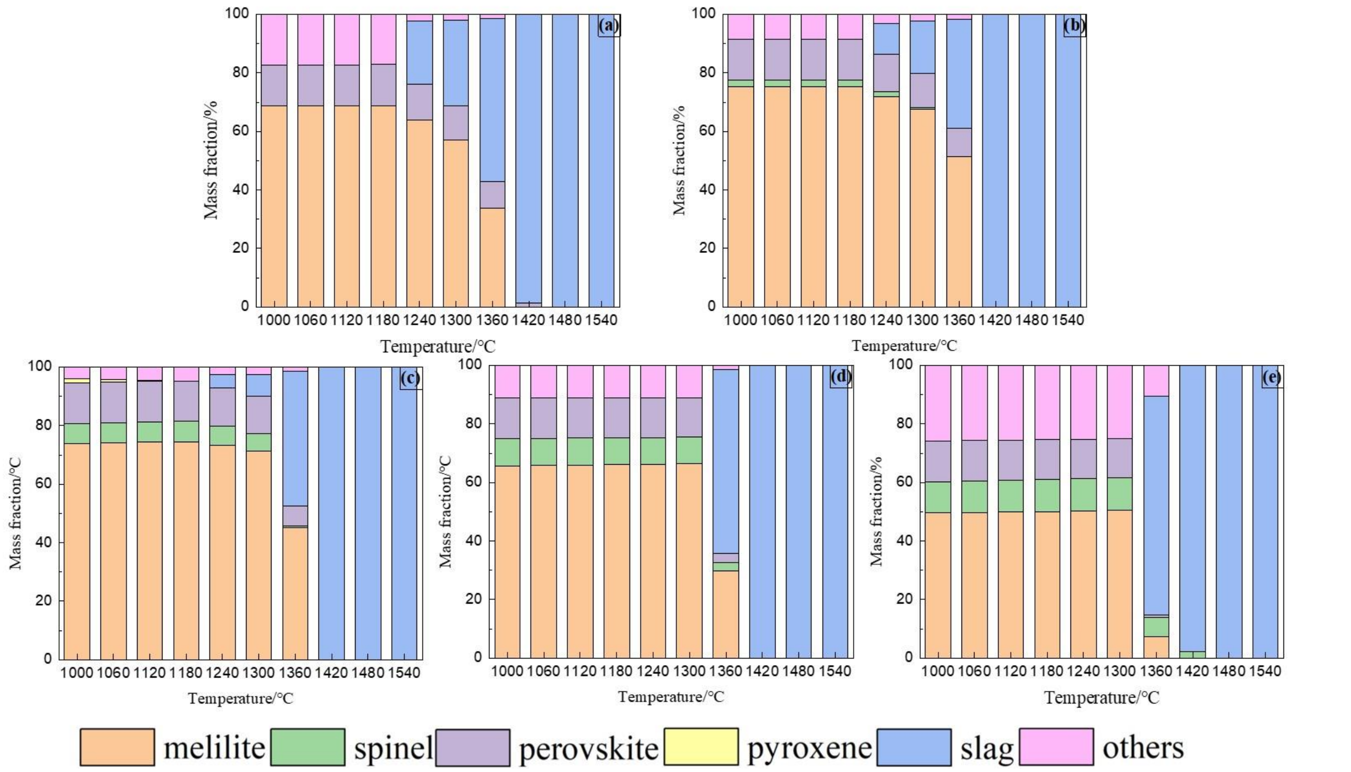

Figure 9. Effect of different MgO content on phase change: (**a**) 6% MgO content, (**b**) 8% MgO content, (**c**) 10% MgO content, (**d**) 12% MgO content, (**e**) 14% MgO content.

4. Conclusions

(1) MgO addition significantly affects the softening-melting behaviors, permeability of V-Ti mixed burden, and the V-Ti slag system. Fully considering the constant total MgO content in composite burden and the softening-melting properties of composite burden, the recommended MgO content in sinter and pellet are 1.90% and 3.02%, respectively.

(2) MgO addition significantly affects the crystallization temperature of slag-phase, precipitated phase components, and molten slag percentages. This indicates that the metallurgi-

cal properties of slag and softening-melting-dripping performance of the mixed burden could be improved effectively by adjusting the MgO distribution appropriately.

(3) The MgO slag system shows the characteristics of short slag. With the increase in MgO content in slag, the melting temperature t_m, initial viscosity η_0, high temperature viscosity η_h, and viscous flow activation energy E_η of the slag system first decrease and then increase, and the thermal stability of the slag system first becomes better and then worse.

Author Contributions: Conceptualization, W.Z. and B.W.; methodology, W.Z.; software, X.Z.; validation, M.C., S.H., and B.W.; formal analysis, H.G.; investigation, S.H.; resources, W.Z.; data curation, X.Z.; writing—original draft preparation, B.W.; writing—review and editing, W.Z.; visualization, X.Z.; supervision, H.G.; project administration, M.C.; funding acquisition, W.Z. All authors have read and agreed to the published version of the manuscript.

Funding: This research was funded by the National Natural Science Foundation of China (U1808212, 52104336), Natural Science Foundation of the Jiangsu Higher Education Institutions of China (20KJB45002), and Postdoctoral Research Foundation of Jiangsu Province (7114451120).

Data Availability Statement: Data are available from the authors upon reasonable request.

Conflicts of Interest: The authors declare no conflict of interest.

References

1. Paunova, R. Thermodynamic study of the reduction of titanium magnetite concentrate with solid carbon. *Metall. Mater. Trans. B* **2002**, *33*, 633–638. [CrossRef]
2. Zhao, W.; Chu, M.S.; Guo, H.W.; Liu, Z.G.; Yan, B.J. Softening–melting–dripping characteristics and evolution mechanism of vanadium-bearing titanomagnetite carbon composite briquette used as novel blast furnace burden. *J. Iron Steel Res. Int.* **2021**, *28*, 1082–1094. [CrossRef]
3. Chen, S.Y.; Fu, X.J.; Chu, M.S.; Li, X.Z.; Liu, Z.G.; Tang, J. Carbothermic Reduction Mechanism of Vanadium-titanium Magnetite. *J. Iron Steel Res. Int.* **2016**, *23*, 409–414. [CrossRef]
4. Tan, P.; Hu, H.P.; Zhang, L. Effects of mechanical activation and oxidation-reduction on hydrochloric acid leaching of Panxi ilmenite concentration. *Trans. Nonferrous Met. Soc. China* **2011**, *21*, 1414–1421. [CrossRef]
5. Zhao, W.; Chu, M.S.; Liu, Z.G.; Wang, H.T.; Tang, J.; Ying, Z.W. High-Temperature Interactions Between Vanadium-Titanium Magnetite Carbon Composite Hot Briquettes and Pellets Under Simulated Blast Furnace Conditions. *Metall. Mater. Trans. B* **2019**, *50*, 1878–1895. [CrossRef]
6. Monakhov, I.N.; Khromov, S.V.; Chemousov, P.I.; Yusfin, Y. The Flow of Vanadium-Bearing Materials in Industry. *Metallurgist* **2004**, *48*, 381–385. [CrossRef]
7. Wang, B. Effect of Vanadium Partitioning of Vanadium Yield in BF Smelting Vanadium Titanomagnetite with Ore-Coke Mixed charging Technic. Master's Thesis, North China University of Science and Technology, Tangshan, China, 2021.
8. He, S.Q.; Sun, H.J.; Tan, D.Y.; Peng, D.Q. Recovery of Titanium Compounds from Ti-enriched Product of Alkali Melting Ti-bearing Blast Furnace Slag by Dilute Sulfuric Acid Leaching. *Procedia Environ. Sci.* **2016**, *31*, 977–984. [CrossRef]
9. Zhao, W.; Chu, M.S.; Wang, H.T.; Liu, Z.G.; Tang, J.; Ying, Z.W. Effect of Introducing Coke into Ore Layer on Softening-melting-dropping Characteristics of Vanadium-titanium Mixed Burden under Simulating BF Conditions. *ISIJ Int.* **2018**, *58*, 1989–1998. [CrossRef]
10. Gao, Q.J.; Jiang, X.; Zheng, H.Y.; Shen, F.M. Induration Process of MgO Flux Pellet. *Minerals* **2018**, *8*, 389. [CrossRef]
11. Fan, J.J.; Qiu, G.Z.; Jiang, T.; Guo, Y.F.; Mu, K.L. Improvement of Sinter Properties with Ultra Fine-Sized Iron Concentrate by HPRG. *J. Iron Steel Res.* **2013**, *20*, 47–52. [CrossRef]
12. Zhang, L.H.; Yang, S.T.; Tang, W.D.; Xue, X.X. Investigations of MgO on Sintering Performance and Metallurgical Property of High-Chromium Vanadium-Titanium Magnetite. *Minerals* **2019**, *9*, 324. [CrossRef]
13. Yang, Y.H.; Lei, T.; Qin, Y.L. Effect of MgO Content on Heat Capacity of Synthetic BF Slag and Heat Release Behavior during Cooling Process. *Metals* **2021**, *11*, 1294. [CrossRef]
14. Xing, X.D.; Pang, Z.J.; Zheng, J.L.; Du, Y.L.; Ren, S.; Ju, J.T. Effect of MgO and K2O on High-Al Silicon–Manganese Alloy Slag Viscosity and Structure. *Minerals* **2020**, *10*, 810. [CrossRef]
15. Wang, G.L.; Kang, J.; Zhang, J.L.; Wang, Y.Z.; Wang, Z.Y.; Liu, Z.J.; Xu, C.Y. Softening–melting behavior of mixed burden based on low-magnesium sinter and fluxed pellets. *Int. J. Miner. Metall. Mater.* **2021**, *28*, 621–628. [CrossRef]
16. Lu, Y.; Shan, R.; Wang, X.; Liu, Q.; Liu, J. Effect of Al2O3, MgO, and CaO/SiO2 on Viscosity of High Alumina Blast Furnace Slag. *Steel Res. Int.* **2016**, *87*, 241–249. [CrossRef]
17. Shigaki, I.; Sawada, M.; Maekawa, M.; Narita, K. Melting Property of MgO Containing Sinter. *ISIJ Int.* **1980**, *66*, 1612–1621. [CrossRef]

18. Yadav, U.S.; Pandey, B.D.; Das, B.K. Influence of magnesia on sintering characteristics of iron ore. *Ironmak. Steelmak.* **2002**, *29*, 91–95. [CrossRef]
19. Pan, F.; Zhu, Q.S.; Du, Z.; Sun, H.Y. Migration Behavior of the MgO and its Influence on the Reduction of Fe3O4–MgO Sinter. *ISIJ Int.* **2018**, *58*, 652–659. [CrossRef]
20. Matsumura, M.; Hoshi, M.; Kawaguchi, T. Improvement of Sinter Softening Property and Reducibility by Controlling Chemical Compositions. *ISIJ Int.* **2006**, *45*, 594–602. [CrossRef]
21. Panigrahy, S.C.; Verstraeten, P.; Dilewijns, J. Influence of MgO addition on mineralogy of iron ore sinter. *Metall. Trans. B* **1984**, *15*, 23–32. [CrossRef]
22. Zhao, W.; Chu, M.S.; Feng, C.; Wang, H.T.; Liu, Z.G.; Tang, J.; Wang, W.P. Effect of MgO addition on the metallurgical properties of the vanadium-titanium pellet with simulating blast furnace conditions. *Ironmak. Steelmak.* **2020**, *47*, 388–397. [CrossRef]
23. Umadevi, T.; Brahmacharyulu, A.; Sah, R.; Mahapatra, P.C.; Prabhu, M. Optimisation of MgO addition in low and high silica iron ore sinter to improve sinter reducibility at JSW Steel Limited. *Ironmak. Steelmak.* **2014**, *41*, 270–278. [CrossRef]
24. Higuchi, K.; Naito, M.; Nakano, M. Optimization of Chemical Composition and Microstructure of Iron Ore Sinter for Low-temperature Drip of Molten Iron with High Permeability. *ISIJ Int.* **2004**, *44*, 2057–2066. [CrossRef]
25. Guo, H.; Shen, F.M.; Zhang, H.Y.; Gao, Q.J.; Jiang, X. High-Temperature Reduction and Melting Mechanism of Sinter with Different MgO Content. *Met.-Open Access Metall. J.* **2019**, *9*, 510. [CrossRef]